Relations between Microstructure and the Fracture Toughness of Metals

G. T. Hahn and A. R. Rosenfield
Battelle, Columbus Laboratories, Columbus, Ohio 43201

1. INTRODUCTION

The origins of fracture toughness of metals can be analyzed by focusing on one or more of the 4 distinct regions that surround the crack tip (see Figure 1a):

The highly distorted lattice ($\sim 10^{-7}$ cm). In this region which is analogous to the dislocation core, large elastic strains, $\epsilon_e \gtrsim 10^{-1}$, are encountered and the linear elastic compliances cease to be meaningful. Among the important structural features are the electron structure (responsible for the interatomic forces), lattice symmetry, and such defects as vacancies, the free surface, and solute atoms.

The region of large plastic stretch (~ 0.001 cm). In this region, which sustains plastic strains $1 \lesssim \epsilon_p \lesssim 10^{-1}$, the microscopic heterogeneities, such as second phase particles, inclusions, local plastic instabilities, and ruptured interfaces enter in an important way. Of particular interest is the interaction of these heterogeneities with the crack tip.

The plastic zone (~ 0.1 cm). In the largest part of the plastic zone plastic strains are moderate $\epsilon_p \lesssim 10^{-1}$, and it is possible to consider the material as an isotropic homogeneous continuum. Microstructural features play an indirect role, either through their influence on such macroscopic quantities as yield strength and work hardening rate or by setting the stage for subsequent instabilities.

The elastically strained region (> 0.1 cm). The region beyond the plastic zone experiences modest elastic strains $\epsilon_e < 10^{-2}$ which are

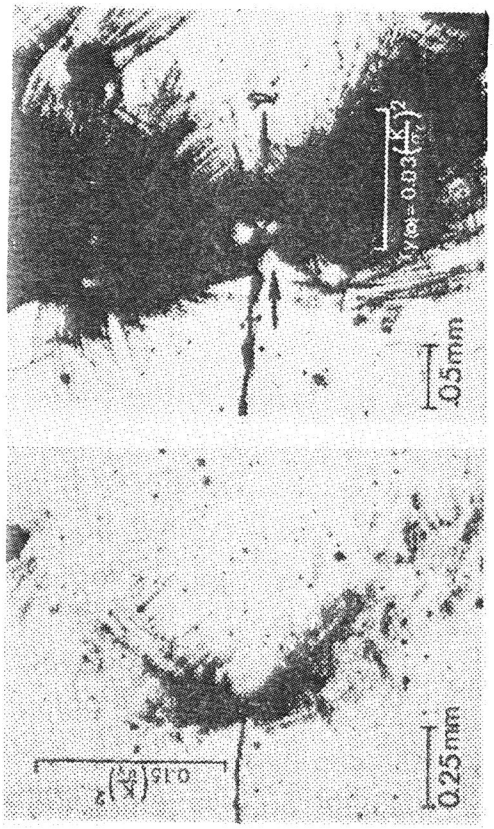

(a) Regions surrounding the crack tip. Dimensions in units of $(K/\sigma_Y)^2$

(b) Plastic zone revealed by etching

(c) Close-up of (b) showing light etching "Region of Large Plastic Stretch" near the crack tip

FIGURE 1. Regions surrounding the crack tip. The plastic zone boundaries shown in (a) are derived from finite element computations by Levy, et al[1]. The plastic zone shown in (b) and (c) was revealed on an interior section of an Fe-3Si steel plate by etching[2]. Lightly deformed regions in (b) etch dark. The three-lobed, light etching zone visible around the close-up of the crack tip in (c) is the region within which plastic strains are greater than ~ 0.1, and corresponds to the "region of large plastic stretch".

described, approximately, by the stress intensity parameter K. Microstructural features are much less important, entering in only through their effect on elastic constants, which is often quite small.

The response of these regions dictates the mode of crack extension in the test piece and the toughness. This paper examines the connection between various fracture toughness indexes (G_c, K_{Ic}, R, and δ^*)† and the events in one or more of the regions for: (i) the cleavage (brittle), (ii) fibrous (ductile), and (iii) cyclic (fatigue) modes of crack extension.

2. CRACK EXTENSION BY CLEAVAGE

2.1 Single Crystals

The toughness of crystals depends initially on the properties of the highly distorted and dilated lattice extending ~ 10^{-7} cm from the

† Indices of Fracture Toughness

Energy conservation dictates that crack extension can only occur when:

$$G \geq R \qquad (1)$$

where G is the energy per unit area released by the cracked structure (strain energy plus external work) during an incremental extension of the crack, and R is the energy per unit area absorbed by the material in the process of crack extension. The energy R is, perhaps, the most direct expression of fracture toughness, but it is difficult to measure. For this reason the toughness is frequently expressed in terms of G_c, which is the minimum value of G at which crack extension is observed experimentally and an indirect measure of R. As an alternative criterion for materials that exhibit large amounts of crack-tip plasticity, some workers advocate the measurement of δ^*, the crack (tip) opening displacement (or COD) at the onset of crack extension. For low toughness materials the quantity K_{Ic}, the critical stress intensity parameter, which contains the fracture energy and the contribution of the elastically strained region near the crack tip, is a more direct measure of the critical load-crack size combination. Since all four toughness indices are closely related:

$$R = G_c = \frac{(1-\nu^2)}{E} K_{Ic}^2 = (1-\nu^2)\, 2\sigma_Y \delta^* , \qquad (2)$$

they are used interchangeably in this paper (E is Young's modulus, ν is Poissons ratio, and σ_Y is the yield stress). A more comprehensive review of these indexes is given in Reference 3.

TABLE 1. FRACTURE TOUGHNESS OF SELECTED METALS AND ALLOYS

Material	Mode of Crack Extension	$2\gamma^{\dagger}$ (J/m^2)	G_c (J/m^2)	K_{Ic} $MNm^{-3/2}$	Reference
Brittle Single Crystals					
Tungsten (-196°C)	Cleavage	5.8[a]	8-12	1.8-2.2	6,7,8
Molybdenum (-269°C)	Cleavage	3.8[b]	6	1.0	9,10
(-196°C)	Cleavage		12	1.5	10
Fe-3Si (-269°C)	Cleavage	3.4-3.8[b]	4.5-9	0.8-1.1	11,12
Beryllium (-192°C)	Cleavage	2.0[c]	4-5	1.1-1.2	13,14
Zinc (-196°C)	Cleavage	1.5[d]	0.2	0.2	15,16
Polycrystalline Alloys					
Low-to-Medium Strength Steels	Cleavage		600-100,000	10-150	17
	Fibrous		200,000-1,000,000	200-500	18
High Strength Aluminum-Base Alloys	Fibrous		5,000-20,000	20-40	19
High Strength Titanium-Base Alloys	Fibrous		10,000-40,000	30-120	20
High Strength Steels	Fibrous		5,000-130,000	30-150	21

† Surface energy values quoted were measured at high temperatures. Values appropriate at the low test temperature are a factor ~ 2 larger.

a. Pulsed field emission (1725°C)
b. Zero creep
c. Gas bubble (725°C)
d. Sessile drop (420°C)

n which reflects the ease of bond shear relative to bond rupture becomes the determining factor. It should be noted that the Griffith and Orowan energy concepts do not define n, but merely its consequences.

The microstructural factors that influence the competition between bond rupture and bond shear at the crack tip are not well understood. From experience: (i) that fcc crystals are generally tough, (ii) that Group VI bcc crystals tend to be more brittle than the Group V bcc, and (iii) that brittleness is influenced by composition, we can infer that ease of bond rupture relative to shear is affected by crystal structure, the nature of the interatomic potential, and by local perturbations in the lattice. Fracture toughness values of brittle single crystals tend to increase rapidly above a certain temperature and, as shown in Figure 3, there is evidence that the increase coincides with the onset of dislocation generation at the crack tip.[12-27] Presumably, bond shear (dislocation generation) is assisted by thermal fluctuations to a greater extent than bond rupture.

A first approximation to the quantitative description of the shear-rupture competition has been obtained from linear elastic models.[28] More detailed approaches, involving the interaction of glide dislocations and the crack tip stress field have been carried out[29,30] but these are still linear elastic and have limited predictive value. Computer simulation offers a means of treating the crack tip as a region of discrete atoms and nonlinear interactions. Using this technique, Gehlen, et al have modeled dislocation generation and crack extension (see Figure 1 of their paper at this conference[31]). Further studies of these computer models are expected to clarify the contributions of the lattice structure, defects, the interatomic potential and thermal fluctuations to the fracture toughness, and the transition temperature of crystals.

2.2 Polycrystalline Materials

Polycrystalline materials, particularly structural steels, also display the transitions from the low-toughness-level cleavage mode of crack extension to higher toughness levels associated with fibrous mode. However, the fracture energy values for cleavage in polycrystalline materials are 3 to 4 orders of magnitude larger than 2γ (see Figure 3). The implication is that many dislocations are generated in the process of cleaving polycrystalline aggregates. Metallographic sections of the profiles of rapidly running brittle fractures, such as the one in Figure 4, reveal that the plastic deformation is not uniformly distributed. Such sections show that the crack extends by relatively brittle cleavage, and that some isolated grains or groups of grains, which fail to cleave at the crack front, are left behind, and act as ligaments.[32] The plastic stretching and rupture of these ligaments behind the crack front appears to be the major energy absorbing process.[32]

Two viewpoints have thus emerged about the mechanism of crack extension by cleavage in polycrystals. One is, that the production of isolated cleavage cracks is relatively easy and that the onset of crack extension is controlled by the intervening ligaments. Krafft[33] first formulated the toughness in this case; an improved approximation has since been derived with the aid of the Dugdale model[32]:

$$K_{Ic} \sim \frac{r}{R}\sqrt{E\sigma_Y v} \qquad (6)$$

where r and R are the average width and spacing of the ligaments, σ_Y and v the yield strength and maximum stretch of the ligament, and E is the elastic modulus of the matrix. Large changes in K_{Ic} for ostensibly 100% cleavage fractures near the transition temperature (see Figure 3) seem to arise both from changes in the number and size of the ligaments and in the ligament stretch[32]. The influence of microstructure on the ligaments has not yet been studied directly. However, there is an empirical correlation between fracture toughness measurements and v-notch Charpy energy[34] at the lower end of the transition range. Consequently, the well-known effects of grain size, carbide morphology, and nickel content on Charpy energy values in the transition temperature range[35] may be connected with the mechanisms by which these elements of the microstructure influence the ligaments. However, quantitative relations between microstructure and ligament formation are not yet available.

The other viewpoint is that crack extension is controlled by the nucleation of isolated cleavage cracks and that ligament rupture follows easily. This view derives support from correlations betwen K_{Ic} and σ^*, the cleavage fracture stress displayed by unnotched bars. Experiments show that the ratio of $\sigma/\sigma^* > 1$ (σ is the maximum normal stress near the crack tip: $\sigma = 2.5\ \sigma_Y$) and increases systematically with decreasing plastic zone size. These correlations are qualitatively consistent with a modified Weibull statistical analysis[36], which relates the probability of finding a favorable cleavage-crack initiation-site, to the stressed (plastic zone) volume. Effects of microstructure on K_{Ic} are through σ^* and σ_Y which depend on grain size, carbide morphology, etc.[37-38] The approach has proven useful for rationalizing temperature and strain rate effects on K_{Ic}[39], but more work is needed to establish that it is soundly based.

3. CRACK EXTENSION BY THE FIBROUS MODE

Crack extension in commercial alloys proceeds more commonly by the "ductile" of "fibrous" mode which displays characteristic "dimples" at high magnification (see Figure 5b). The term "ductile" is sometimes a misnomer because "fibrous" crack extension can proceed with fracture toughness values below the levels encountered for cleavage (see Table 1).

Metallographic studies of unnotched tensile bars, whose fracture surfaces also display the fibrous, dimpled appearance show that the failure process involves the following sequence illustrated in Figure 5a: (i) plastic deformation of the matrix, (ii) the fracture of hard particles within the ductile matrix, either by cleavage or by separation at the particle-matrix interface, (iii) the growth of the voids produced by these failures, and (iv) the coalescing of voids and their joining with the main crack front. The individual hemispherical voids surrounded by drawn-out ligaments give the fracture the fibrous, dimpled appearance. Several workers have treated void growth and coalescence in a continuum[40,42,43]. These analyses indicate that the fracture strain is a function of the volume fraction of the initial void array and the triaxiality of stress. The same result has been obtained with experiments on unnotched bars with varying volume fraction of particles, notably by Edelson and Baldwin[45], and others[46-50]. As shown in Figure 6, the fracture strain correlates with the volume fraction of cracked particles,

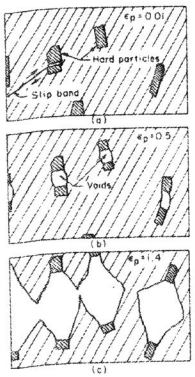

(a) Schematic of void nucleation, growth and coalescing

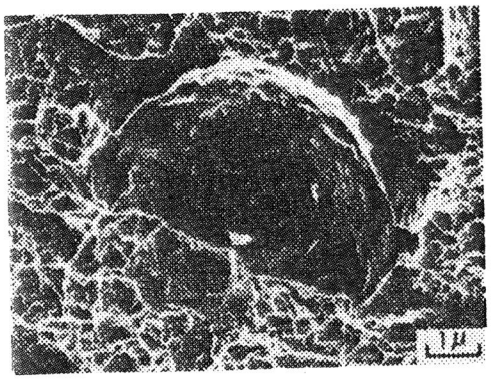

(b) Fracture surface produced by unstable crack extension in quenched and tempered 4340 steel. Large dimple identified with MnS, small dimples with cementite[56]

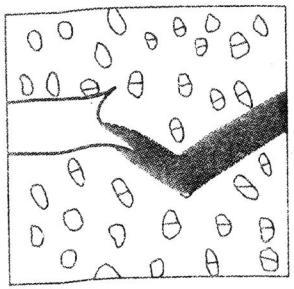

(c) Plastic instability (grey band) within region of large plastic stretch[40,43]

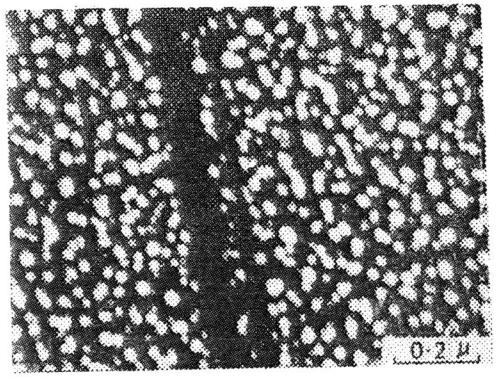

(d) Evidence of particle breakdown within a slip band of Ti8Al alloy[4]

Figure 5. Mechanism of Fibrous Crack Extension

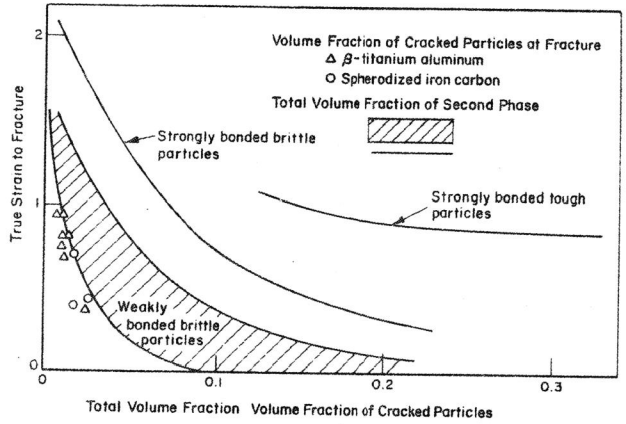

Figure 6. Influence of volume fraction of second phase particles on the fracture strain of unnotched tensile bars.[3]

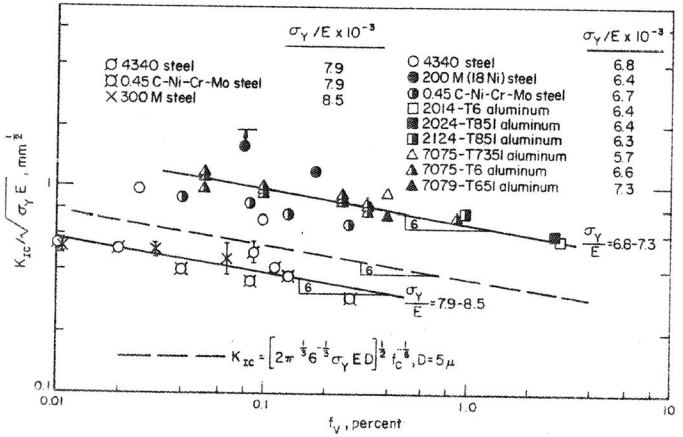

Figure 7. Influence of volume fraction of cracked second phase particles on K_{Ic}[55-59]. It is assumed that all of the particles of the weak phases, identified in Table 2, below, cracked ($f_v = f_c$).

TABLE 2. IDENTITY OF CRACKED SECOND PHASE PARTICLES

Material	Cracked Phase	Reference
4340 Steel	MnS	55
0.45C-NiCr-Mo Steel	MnS	58
300M Steel	MnS, $CaO \cdot 6Al_2O_3$, Ti(C,N)	59
200M (18Ni) Steel	Ti(C,N)	55
2014-T6 Aluminum	$Al_4CuMgSi_4$, $Al_{12}(FeMn)_3$	56
2024-T851 Aluminum	$Al_2Cu(Mn,Fe)_3$, $CuAl_2$	56
2124-T7351 Aluminum	$Al_{20}Cu_2(Mn,Fe)_3$	56
7075-T7351 Aluminum	$(Fe,Mn,Cu)Al_6$	56
7079-T651 Aluminum	$(Fe,Mn,Cu)Al_6$	56

rather than with the total volume fraction of the second phase and three types of particles can be distinguished:

Weakly Bonded Brittle Particles. Power metallurgy products containing oxides and iron containing sulfides are examples of systems that form void nuclei at the particle/matrix interface immediately at the onset of straining because the particles are weakly bonded to the matrix. In these systems the volume fraction of cracked particles and the total volume fraction of second phase nearly coincide (see Figure 6).

Strongly Bonded Brittle Particles. Iron with spherodized carbides is a typical example. Here void nucleation is cumulative, so that for a given volume fraction of particles, there are always fewer voids than particles.

Strongly Bonded Tough Particles. In systems like β Ti-Al containing deformably α Ti-Al, only a small part of the total volume fracture of α-particles is ever cracked.

Accordingly, a given volume fraction of second phase can be more or less deleterious depending on the resistance of the particles to decohesion and cracking.

During crack extension, hole growth and coalescence must proceed in the heavily strained region of the plastic zone. Rice and Johnson[51] have shown that large deformations are confined to a very small "region of large plastic stretch" whose extent is comparable to δ, the crack (tip) opening displacement, which is typically an order of magnitude smaller than $r_{Y(0)}$ the furthest extent of the plastic zone directly in front of the crack. As given in Reference (2),

$$\delta \approx 0.5 \frac{K^2}{E\sigma_Y} \approx \frac{17\ \sigma_Y\ .\ r_{Y(0)}}{E} \qquad (7)$$

Figure 1 defines the dimensions $r_{Y(0)}$ and δ and shows a plastic zone and region of large plastic stretch revealed by etching.

Beginning with Krafft[52], various attempts have been made to formulate the process of hole growth within the region of large plastic stretch including detailed continuum elastic-plastic analyses by McClintock,[53] Thomasson[54], and Rice and Johnson[51]. From a metallurgical point of view, the following approximate failure criterion proposed by Rice and Johnson[51] is instructive: crack extension proceeds when δ, the extent of the heavily stretched region is comparable to the width of the unbroken ligaments which is approximated by λ_c, the spacing of cracked particles:

$$\lambda_c \approx \delta^* \ . \qquad (8)$$

The quantity, δ^* can be related to other toughness indices by way of Equation (2)

$$K_{Ic} \approx \sqrt{2\sigma_Y E \lambda_c} \qquad (9)$$

These relations can also be restated in terms of f_c, the volume fraction of cracked particles†:

$$K_{Ic} \approx \left[2\sigma_Y E \left(\frac{\pi}{6}\right)^{1/3} D\right]^{1/2} f_c^{-1/6} \qquad (10)$$

where D is the particle diameter. Figure 7 illustrates that experimentally measured K_{Ic}-values do tend to display a 1/6th-power dependence on volume fraction and that the values given by Equation (10) are of the right order of magnitude.†† The cracked second phase particles in these alloys are identified in Table 2.

The major shortcoming of this and similar analyses is that they fail to predict the loss of fracture toughness with increasing

† The spacing of an array of particles is a function of f_v, the volume fraction of the second phase. For the idealized case of a regular cubic array of uniform spherical particles: $S = A\ f_v^{-1/3}$ and $A^3 = \frac{\pi}{6} D^3$, where D is the particle diameter.

†† The weak dependence of K_{Ic} on D predicted by Equation (10) does not seem to be observed in practice.

yield strength level which makes the highest strength structural alloys exceedingly flaw sensitive. This is shown in Figure 7, which reveals that $K_{Ic}/\sqrt{\sigma_Y E}$ is not independent of yield strength for constant volume fraction and modulus (as predicted by Equation (10)), but that the highest strength steels display consistently lower toughness values. This loss of toughness is associated with the presence of plastic instabilities within the region of large plastic stretch along the line proposed by McClintock[43] and Berg[40]. Figure 5c illustrates the concept schematically: the instabilities tend to confine shear into narrow bands and, by intensifying strain locally, accelerate the linking of voids. They also provide a mechanism for re-sharpening the crack prior to final fracture. Several recent studies lend weight to this idea. Cox and Low[55] find that the large dimples produced by the fracture of MnS inclusions in 4340 steel are connected by much smaller dimples associated with the cementite particles which strengthen this steel. No small dimples were resolved on specimens of an 18Ni-200 maraging grade which is substantially tougher for the same volume fraction of inclusions. Broek[60] has interpreted observations that dimples associated with intermediate-size dispersoids in aluminum alloys are shallow; evidence that small voids connect by shearing. Clausing[61] and the present authors[62] have found that unusually coarse deformation bands, which crack prematurely, are a common feature of high strength alloys deformed under plane strain conditions. Taken together, these studies suggest (i) the linking up of large voids is assisted by plastic instabilities, (ii) the instabilities are a consequence of the slip induced breakdown of submicron-size particles that strengthen the alloys, and (iii) the breakdown occurs more rapidly at higher strength levels where the particles are smaller and more fragile. This hypothesis cannot be supported in any detail, but it is interesting to note that Boyd[41] has obtained evidence

of the deterioration of fine particles in a slip band (see Figure 5d).

4. CRACK EXTENSION BY CYCLIC GROWTH

The successive loading and unloading of a crack (to subcritical-K levels) can be expected to produce small forward and backward movements of the crack front comparable in magnitude to δ†. Laird[63] and McClintock[64] first suggested that fatigue crack growth is a consequence of an "irreversibility" or "damage" which prevents the complete recovery of the forward motion during the unloading cycle. The per-cycle crack advance (or crack growth rate), $\frac{da}{dn}$ can be expressed in terms of other material properties provided the irreversibility is proportional to $\Delta\delta$ (see footnote)[66,67]:

$$\frac{da}{dn} = A\,\Delta\delta = \frac{0.25A\Delta K^2}{E\sigma_Y{}^c} \qquad (11)$$

where A is the proportionality factor. Equation (11) comes close to describing crack growth behavior with one notable exception: crack growth rates are insensitive to large changes in the yield strength![68] It appears that the usual microstructural alterations that affect σ_Y and $\sigma_Y{}^c$) may also be altering the factor A.

Recent studies of $\Delta\delta$[69] and the plastic zone of a fatigue crack[70,71] lend support to the approximate description of the cyclic strain history experience by material ahead of a fatigue crack reproduced in Figure 9. The pattern of straining in the preyield and cyclic plastic zone regions would be expected to produce a dipole-rich fatigue-type substructure,[72] and this has been confirmed by transmission studies[73]. Other evidence suggests that the last 5-10 cycles, which involve very

† The plastic stretch δ (see Figure 1a) must be accompanied by a contraction at the root of the crack comparable to δ, because plastic deformation proceeds at constant volume. Estimates of the magnitude of $\Delta\delta$ and $r^c_{Y(D)}$, the cyclic variation of δ and the cyclic plastic zone size, can be obtained by replacing σ_Y with $2\sigma_Y{}^c$, where $\sigma_Y{}^c$ is the cyclic yield stress[65]. An example of a cyclic plastic zone revealed by etching is given in Figure 8.

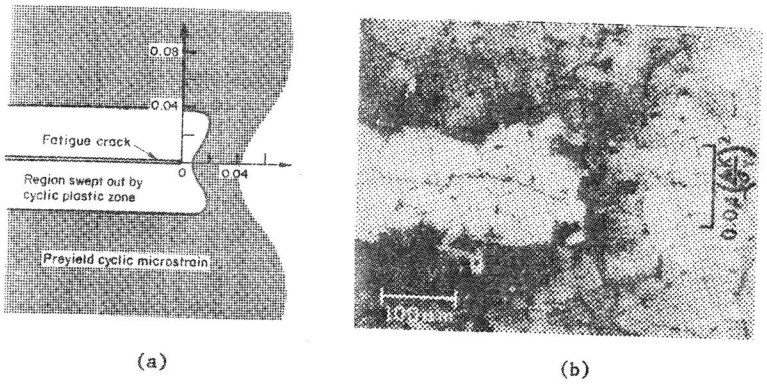

(a) (b)

Figure 8. The fatigue crack plastic zone: (a) schematic, scale in units of $\left(\frac{\Delta K}{\sigma_Y}\right)^2$, (b) zone revealed in the interior of an Fe-3Si steel plate[70]. Region swept out by cyclic plastic zone is light etching, region that has experienced preyield cyclic microstrain is dark etching.

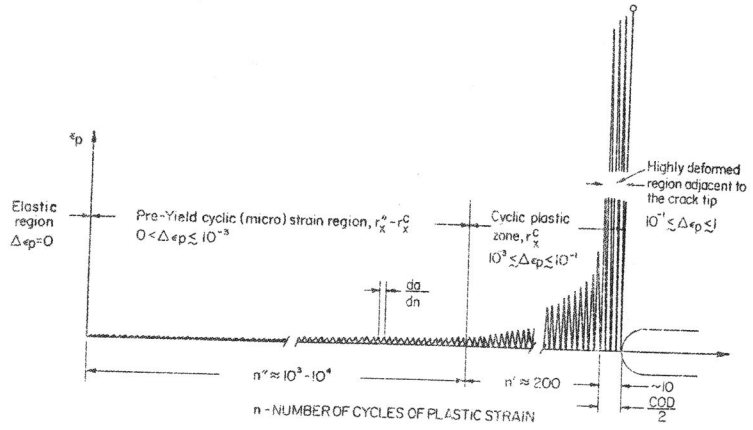

Figure 9. Cyclic strain history experienced by material in advance of a fatigue crack[69,70]

large increments of strain per cycle, may then "unravel" the substructure, a process that could contribute to irreversibility. This idea suggests that the stability of the fatigue substructure influences fatigue crack growth. The argument derives support from the work of Miller and coworkers[74], and more recently, by Ishii and Weertman[75], who altered the substructure by (i) alloying copper with up to 13.5% aluminum, which reduces the stacking fault energy from 40 ergs/cm^2 to 2.5 ergs/cm^2, and (ii) lowering the test temperature from room temperature to -196°C, which probably reduces cross slip. These changes, which are known to alter the fatigue substructure[72] produced as much as a 15-fold reduction in the fatigue crack growth rate.[75]

5. CONCLUSIONS

5.1 Cleavage Crack Extension

The fracture toughness of brittle single crystals that fail by cleavage is determined by the elastic moduli and the specific surface energy of the cleavage plane. The fracture energy of crystals can be orders of magnitude greater when bond shear (dislocation generation and motion) precedes bond rupture at the crack tip. The competition between bond shear and rupture is influenced by microstructural elements on the atomic scale: the crystal lattice, the interatomic forces at large displacements, thermal fluctuations and lattice defects. The fracture toughness of polycrystalline materials that cleave, such as structural steels, depends on the cleavage toughness of the individual crystals, and on isolated grains (ligaments) which fail to cleave immediately and rupture after absorbing additional energy. The microstructure: grain size, carbide morphology, etc., influences cleavage initiation and, possibly, the ligament spacing and ligament stretch.

5.2 Fibrous Crack Extension

Toughness values for the fibrous mode depend on the volume fraction of weak second phase particles and inclusions and on the requirements for rupturing the matrix between the particles which involves the modulus and yield strength of the alloy. The volume fraction of second phase is more or less deleterious depending on the particles' resistance to decohesion and cracking. The linking up of the voids produced by the particles may be assisted by localized plastic instabilities and by the slip-induced breakdown of the submicron-size particles in high strength alloys.

5.3 Cyclic Crack Growth

The resistance to cyclic crack growth (fatigue) is roughly proportional to the elastic modulus. It is also influenced by the stacking fault energy and other variables that influence the dislocation substructure generated by cyclic straining within the plastic zone.

ACKNOWLEDGMENTS. The authors are indebted to the AF Aerospace Research Laboratory, the AF Materials Laboratory, the Office of Naval Research, and the Ship Structure Committee who have supported research on this topic. They wish to thank R. Hoagland, M. Kanninen, and P. Gehlen for stimulating discussions and acknowledge the important contributions of P. Mincer, R. Barnes, and C. Pepper.

REFERENCES

1. N. Levy, P. V. Marcal, W. J. Ostergren, and J. R. Rice, Int. J. Fract. Mech., Vol. 7, p. 143, 1971.
2. G. T. Hahn and A. R. Rosenfield, Ship Structure Committee, Report SSC-191, 1968.
3. G. T. Hahn, M. F. Kanninen, and A. R. Rosenfield, Ann. Rev. Mat. Sci., Vol. 2 (in press).
4. A. R. Griffith, Phil. Trans. Royal Soc., Vol. A221, p. 163, 1920.
5. E. D. Hondros, Physicochemical Measurements in Metals Research, Part 2, ed., R. A. Rapp; Wylie, New York (1970), p. 293.
6. J. P. Barbour, F. M. Charbonnier, W. W. Dolan, W. P. Dyke, E. E. Martin, and J. K. Trolan, Phys. Rev., Vol. 117, p. 1452, 1960.
7. J. E. Cordwell and D. Hull, Mag., Vol. 19, p. 951, 1969.

8. J. E. Cordwell and D. Hull, Phil. Mag., Vol. 26, p. 215, 1972.
9. B. C. Allen, J. Less Common Metals, Vol. 17, p. 403, 1969.
10. P. Beardmore and D. Hull, Refractory Metals and Alloys IV, eds. R. I. Jaffee, et al; Gordon & Breach (1967), p. 81.
11. E. D. Hondros and L.E.H. Stuart, Phil. Mag., Vol. 17, p. 711, 1968.
12. R. Pilkington and D. Hull, Iron & Steel Inst., Pub. 120, p. 5, 1970.
13. R. S. Barnes and B. G. Redding, J. Nucl. Energy, Vol. 10, p. 32, 1959.
14. R. G. Govila and M. H. Kamdar, Met. Trans., Vol. 1, p. 1011, 1970.
15. D.W.G. White, Trans AIME, Vol. 236, p. 796, 1966.
16. A.R.C. Westwood and M. H. Kamdar, Phil. Mag., Vol. 8, 787, 1963.
17. G. T. Hahn, R. G. Hoagland, and A. R. Rosenfield, Met. Trans., Vol. 2, p. 537, 1971.
18. G. T. Hahn, M. Sarrate, and A. R. Rosenfield, Int. J. Fract. Mech., Vol. 5, 187, 1969.
19. F. G. Nelson and J. G. Kaufman, ASTM STP 496, p. 27, 1971.
20. C. N. Freed, Eng. Fract. Mech., Vol. 1, p. 175, 1968.
21. G. E. Pellesier, Eng. Fract. Mech., Vol. 1, p. 55, 1968.
22. J. J. Gilman, Trans AIME, Vol. 209, p. 449, 1957.
23. E. Orowan, Reports Prog. Phys., Vol. 12, p. 185, 1948.
24. J. Friedel, Fracture, eds. B. L. Averbach, et al, MIT, Cambridge (1959), p. 498.
25. A.R.C. Westwood, C. M. Preece, and M. H. Kamdar, Fracture, ed. H. Liebowitz, Academic Press, N.Y., Vol. 3 (1971), p. 589.
26. P. C. Gehlen, G. T. Hahn, and A. R. Rosenfield, N.B.S. Spec. Pub. 317 [1], p. 305, 1970.
27. R. K. Govila, Acta Met, Vol. 17, p. 1209, 1969.
28. A. Kelly, W. R. Tyson, And A. H. Cottrell, Phil. Mag., Vol. 15, p. 567, 1967.
29. S. J. Burns and W. W. Webb, Trans AIME, Vol. 236, p. 1165, 1966.
30. R. Ayers and D. F. Stein, Acta Met, Vol. 19, p. 789, 1971.
31. P. C. Gehlen, G. T. Hahn, and M. F. Kanninen; this volume.
32. R. G. Hoagland, A. R. Rosenfield, and G. T. Hahn, Met Trans, Vol. 3, p. 123, 1972.
33. J. M. Krafft, Appl. Mater. Res., Vol. 3, p. 88, 1964.
34. S. T. Rolfe, ASTM STP 463, p. 188, 1970.
35. F. W. Boulger, Fracture, ed. H. Liebowitz, Vol. 6, (1968), p. 181.
36. K. G. Hanson and W. G. Forsman, Appl. Polym. Sci., Vol. A2, p. 7, 1969.
37. W. E. Duckworth and J. D. Baird, J. Iron Steel Inst., Vol. 207, p. 854, 1969.
38. A. R. Rosenfield, G. T. Hahn, and J. D. Embury, Met. Trans (in press).
39. G. T. Hahn, R. G. Hoagland, and A. R. Rosenfield, Met. Trans, Vol. 2, p. 537, 1971.
40. C. A. Berg, Inelastic Behavior of Solids, M. F. Kanninen, et al, eds., McGraw-Hill, N.Y. (1970), p. 171.
41. J. D. Boyd, Dept. of Energy, Mines, & Resources, Ottawa, private communication (1972).
42. D. M. Tracey, Engg. Fract. Mech., Vol. 3, p. 301, 1971.
43. F. A. McClintock, J. Appl. Mech., Vol. 35, p. 363, 1968.
44. P. F. Thomasson, J. Inst. Met., Vol. 96, p. 360, 1968.
45. B. I. Edelson and W. M. Baldwin, Jr., Trans ASM, Vol. 55, p. 230, 1962.
46. W. S. Cremens and N. J. Grant, Proc. ASTM, Vol. 58, p. 714, 1958.
47. H. Margolin, P. A. Farrar, and M. A. Greenfield, The Science Technology & Application of Titanium, eds. R. I. Jaffee & N. E. Promisel, Pergamon, Oxford, p. 795 (1970).

48. C. T. Liu and J. Gurland, Trans ASM, Vol. 61, p. 157, 1968.
49. V. A. Tipnis and N. A. Cook, Trans ASME, Vol. 89D, p. 533, 1967.
50. L. Roesch, Mem. Sci. Rev. Met., Vol. 66, p. 29, 1969.
51. J. R. Rice and M. A. Johnson, Inelastic Behavior of Solids, eds. M. F. Kanninen, et al., McGraw-Hill, N.Y., p. 641 (1970).
52. J. M. Krafft, Rep. NRL Progr. (1963), p. 4.
53. F. A. McClintock, S. M. Kaplan, and C. A. Berg, Int. J. Fract. Mech., Vol. 2, p. 615, 1966.
54. P. F. Thomasson, Int. J. Fract. Met., Vol. 7, p. 409, 1971.
55. B. Cox and J. R. Low, Jr., Tech. Rep. #3, NASA Grant NGR-39-087-003, 1972.
56. J. R. Low, Jr., R. H. VanStone, and R. H. Merchant, Tech. Rep. #2, NASA Grant NGR-39-087-003, 1972.
57. J. H. Mulherin and H. Rosenthal, Met. Trans., Vol. 2, p. 427, 1971.
58. A. J. Birkle, R. P. Wei, and G. E. Pellisier, Trans ASM, Vol. 59, p. 981, 1966.
59. J. J. Hauser and M.G.H. Wells, Report AFML-TR-69-339, Wright-Patterson AFB, Ohio, 1970.
60. D. Broek, Proefschrift, Technisch Hogeschool Delft (1971).
61. D. P. Clausing, Report 35.066-001(2), U.S. Steel Corp., 1972.
62. G. T. Hahn and A. R. Rosenfield (unpublished research).
63. C. Laird, ASTM-STP-415, p. 131, 1967.
64. F. A. McClintock, Fracture of Solids, eds. D. C. Drucker and J. J. Gilman, John Wiley, N.Y., p. 65 (1963).
65. J. R. Rice, ASTM-STP 415, p. 247, 1967.
66. F. A. McClintock, ASTM-STP 415, p. 170, 1967.
67. R.M.N. Pelloux, Trans ASM, Vol. 62, p. 281, 1969.
68. G. T. Hahn, M. Sarrate, and A. R. Rosenfield, Proc. AF Conf. on Fatigue and Fracture of Aircraft Struct's. and Matl's., AFFDLTR-70-144, p. 425, September, 1970.
69. C. Q. Bowles, Final Tech. Report for AMMRC, AMMRC CR 70-23, June, 1970.
70. G. T. Hahn, R. G. Hoagland, and A. R. Rosenfield, Met. Trans., Vol. 3, p. 1189, 1972.
71. C. Bathias and R. Pelloux, MIT Report, March, 1972.
72. C. E. Feltner and C. Laird, Acta Met., Vol. 15, p. 1633, 1967.
73. M. A. Wilkins and G. C. Smith, Acta Met., Vol. 18, p. 1035, 1970.
74. G. A. Miller, D. H. Avery, and W. A. Backofen, Trans AIME, Vol. 236, p. 1667, 1966.
75. H. Ishii and J. Weertman, Northwestern U. Tech. Report No. 10, NR031-825, September, 1971.